Science in China Ser D: Earth Sciences

Geochemistry and spatial distribution of OIB and MORB in A'nyemaqen ophiolite zone: Evidence of Majixue-shan ancient ridge-centered hotspot

GUO AnLin[1†], ZHANG GuoWei[1], SUN YanGui[1,2], ZHENG JianKang[2], LIU Ye[1] & WANG JianQi[1]

[1] National Key Lab of Continental Dynamics, Northwest University, Xi'an 710069, China;
[2] Qinghai Institute of Geological Survey, Xining 810012, China

The mafic volcanic association is made up of OIB, E-MORB and N-MORB in the A'nyemaqen Paleozoic ophiolites. Compared with the same type rocks in the world, the mafic rocks generally display lower Nb/U and Ce/Pb ratios and some have Nb depletion and Pb enrichment. The OIB are LREE-enriched with $(La/Yb)_N$ =5—20, N-MORB are LREE-depleted with $(La/Yb)_N$ = 0.41—0.5. The OIB are featured by incompatible element enrichment and the N-MORB are obviously depleted with some metasomatic effect, and E-MORB are geochemically intermediated. These rocks are distributed around the Majixue-shan OIB and gabbros in a thickness greater than a thousand meters and transitionally change along the ophiolite extension in a west-east direction, showing a symmetric distribution pattern as centered by the Majixueshan OIB, that is, from N-MORB, OIB and E-MORB association in the Dur'ngoi area to OIB in the Majixueshan area and then to N-MORB, OIB and E-MORB assemblage again in the Buqing-shan area. By consideration of the rock association, the rock spatial distribution and the thickness of the mafic rocks in the Majixueshan, coupled with the metasomatic relationship between the OIB and MORB sources, it can be argued that the Majixueshan probably corresponds to an ancient hotspot or an ocean island formed by mantle plume on the A'nyemaqeh ocean ridge, that is the ridge-centered hotspot, tectonically similar to the present-day Iceland hotspot.

A'nyemaqen ophiolite zone, OIB, N-MORB and E-MORB association, spatial distribution, Majixueshan ridge-centered hotspot, metasomatism, mantle plume

Coexistence of normal mid-ocean-ridge basalts (N-MORB), enriched mid-ocean-ridge basalts (E-MORB) and ocean island basalts (OIB) in the certain tectonic setting has drawn extensive attention and strong interest. Iceland in the North Atlantic Ocean has become a well-known example for the phenomenon. The phenomenon has been thought to be a result of superposition of a hotspot on a ridge (ridge-centered hotspot)[1] or an oceanic island on a ridge (ridge-centered island)[2] or a mantle plume on a ridge (plume on-ridge)[3], and hotspot-ridge interaction or plume-ridge interaction[4,5]. The spatial superposition and materials interaction between a ridge and a hotspot or an ocean island or a plume cause anomalies of geochemistry, topography, crustal structure, gravity, seismic velocity and bathymetry in the area surrounding a ridge-hotspot[1].

Recent studies have indicated that the coexistence not only occurs in a modern environment like Iceland, but also can be traced into ophiolite zones representing preserved oceanic crust in continental orogenic belts. Hou et al.[6,7], according to the coexistence of OIB, N-MORB and T-MORB and their specific configuration in space, proposed a paleo-Tethyan mantle plume model to inter-

Received October 28, 2005; accepted January 10, 2006
doi: 10.1007/s11430-007-0197-3
†Corresponding author (email: anlingxb@nwu.edu.cn)
Supported by the National Natural Science Foundation of China (Grant Nos. 40234041 and 40572138)

pret the formation and evolution of the paleo-Tethys Oceanic crust in the Sanjiang region. In study of magmatic activities in the Qinling orogenic belt, Zhang[8] found that E-MORB (or T- and P-MORB) and OIB in the ophiolite zones of different ages are developed in the northern Qinling, the Southern Qinling and on the northern margin of the Yangtze plate since Proterozoic, and suggested that they are related to mantle plume activities. The association of these rocks and N-MORB together represent typical oceanic crust and also implies existence of the Iceland-like tectonic setting.

OIB and E-MORB have been identified in mafic rocks of different portions in the A'nyemaqen ophiolite zone during the 2003-2004 research work of the key project "Formation, evolution and continental dynamics of the western Qinling-Songpan tectonic node" funded by the National Natural Scientific Foundation. These rocks and N-MORB together are remnants of paleo-oceanic crust and also reveals the peculiar tectonic environment for the occurrence of the paleo-oceanic crust. On the basis of the previous studies, this work attempts to explore their tectonic significance and mantle dynamics at depth by means of lithological geochemistry, rock spatial distribution and the genetic link between the OIB and the coexisting N-MORB. Since the modern Indian Ocean and the paleo-Tethyan Ocean share the same mantle[9], the comparison between rocks in the study area and the Indian Oceanic basalts and the relevant rocks in the Sanjiang region in China will be carried out.

1 Regional geology

The A'nyemaqen ophiolite mélange zone is the eastern extension of the ophiolite belt on the southern margin of the eastern Kunlun Mountains. The mélange zone stretches more than 400 km from east to west in a width of near 100 km, the ophiolites inside the mélange zone are about 3 km wide. To the north, the zone is separated by the east Kunlun fault from the east Kunlun massif and to the south, it borders with the Bayankala-Songpan-Garzê massif along the Changshitoushan fault. Tectonically, the A'nyemaqen ophiolite mélange zone is situated in between the western Qinling-eastern Kunlun orogen and the Yangtze plate, and represents the west-extended constitution of the Mianlue suture zone[10] (Figure 1).

The A'nyemaqen ophiolite zone in NWW-strike consists mainly of Dur'ngoi, Majixueshan and Buqingshan ophiolite occurrences from east to west. The Buqingshan ophiolites in the west is distributed between the Lake Tuosuo and the Dongdatan area. The ophiolites contain the Ordovician and the early Carboniferous-early Permian ophiolitic components[11]. The late-Paleozoic ophiolites are outcropped to southwest of the early-Paleozoic one. Characterized by discontinuous distribution in the general strike, the ophiolites occur in the form of tectonic slices with a diameter of a few tens to about one hundred meters and sandwich in the tectonic blocks comprising the Carboniferous Maerzen clastic limestone and clastic sedimentary rocks. The tectonic blocks are exposed at interval of a few hundred meters. The ophiolites are made up of mafic pillow lava and massive lava with thin-layered radiolarian silicalites. Compared with the Dur'ngoi ophiolites in east, there are less ultramafic rocks exposed in the area. Most pillows are in size of a few tens centimeters, accompanying with carbonate and episode veins as well as greenschist facies metamorphism. Bian et al.[11] reported N-MOREB and minor T-MORB in the Buqingshan late-Paleozoic ophiolites and suggested that they represent an environment of the paleo-Tethyan oceanic basin.

The Dur'ngoi ophiolites belong to the eastern portion of the A'nyemaqen ophiolite zone and are exposed between the lower Permian clastic sedimentary rocks and a suite of supercrust rocks (marbles, amphibolites and schists) of the Proterozoic Dakendaban Formation. A few-tens-meter-wide mylonite zone with intrusions of gabbro and granite veins is developed between the ophiolites down south and the Dakendaban Formation to the north. The tectonic slices of Dur'ngoi ophiolites mainly comprise serpentinized and carbonatized ultramafic rocks with minor metamafic rocks in greenschist facies metamorphism. Relative to the Buqinshan ophiolites, the Dur'ngoi ophilites are structurally reworked. Geochemically, the metamafic rocks of the Dur'ngoi ophiolites are of N-MORB and thought to be the remnants of the paleo-Tethyan oceanic crust[12,13].

The middle portion of the A'nyemaqen ophiolite zone is represented by the Majixueshan ophiolites. In the early 1990s, Jiang et al.[14] discovered about 1000-m-thick mafic lava in the area. The thick-layered lava is characterized by pillow, amygdaloidal and vesicular structures. The pillows are mostly in size of a few tens centimeters to one meter. The lava contains blocks of ultramafic rocks and gabbros as well as silicalite layers

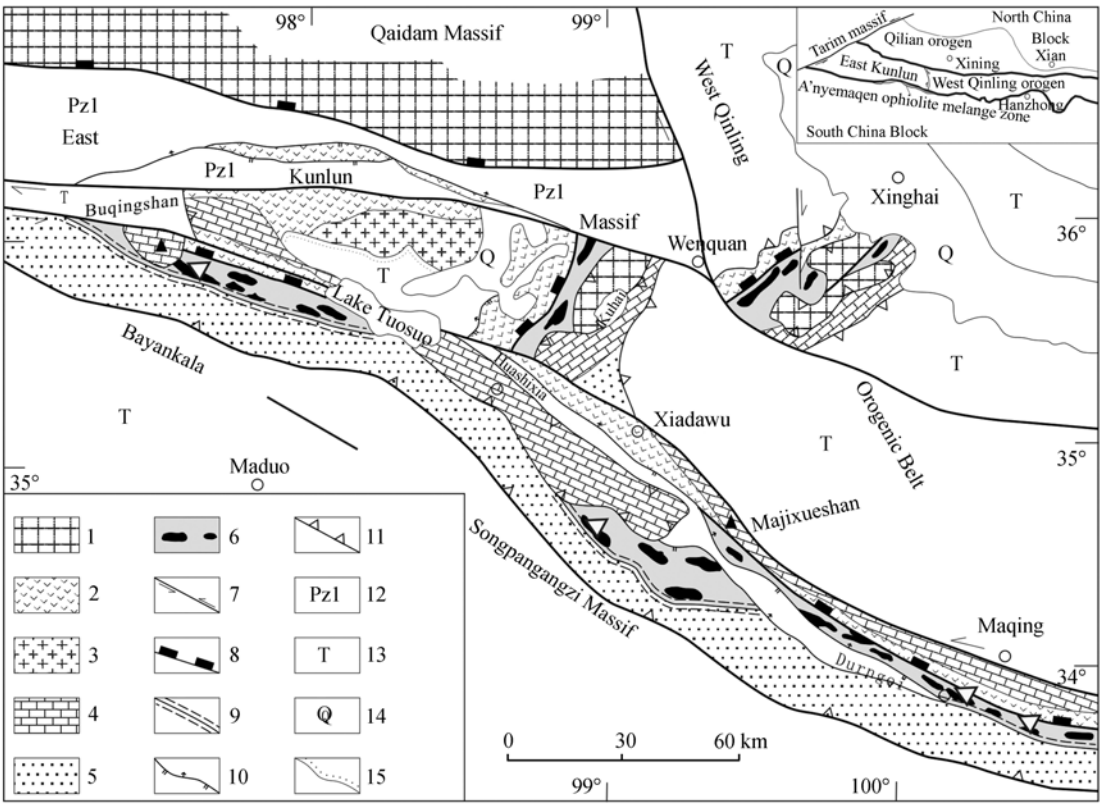

Figure 1 A'nyemaqen ophiolite mélange zone and sketch geological map. 1, Precambrian basement; 2, late Late-Paleozoic volcanic arc system; 3, late Late-Paleozoic collisional granite; 4, Carboniferous-Permian carbonate; 5, flysch deposition on Permian passive continental margin; 6, late-Paleozoic ophiolites; 7, strike-slip fault; 8, subduction zone; 9. ductile fault; 10, thrust faults; 11, nappes; 12, volcano-sedimentary system on early-Paleozoic continental margin; 13, flysch deposition in Triassic foreland basin; 14, Quaternary; 15, anglar unconformity boundary; △, sampling site.

(as thick as 5 cm) and tectonic slabs of Carboniferous and Permian limestone. Affinity to OIB has been indicated for the mafic lava by lithological geochemistry[14]. In addition, about 1000-m-thick basaltic lava and stratiform gabbros are exposed in the Qianliwalima area to southwest of the Majixueshan area. The lava is mainly distributed in the western part of the occurrence and changes into gabbros eastwards. The rocks are commonly subjected to greenschist facies metamorphism in which the dark minerals are substituted by chlorites and episodes, amphiboles can be seen locally.

The previous geochronological studies of the A'nyemaqen ophiolites indicate that the major portion of the ophiolites is the oceanic crust formed in the late Paleozoic. Bian et al.[11] identified early-late Carboniferous siliceous radiolarian from silicalites in the Buqingshan ophiolites. Chen et al.[15] determined a whole-rock $^{40}Ar/^{39}Ar$ plateau age of 345.3 ± 7.9 Ma from basalts in the Dur'ngoi ophiolites. Later, Zhang et al.[16] reported the discovery of early Permian siliceous radiolarian in the Buqingshan ophiolite mélange. Yang et al. obtained a zircon SHRIMP age of 308.2 ± 4.9 Ma from basaltic lava in the Dur'ngoi ophiolites[13]. From regional geology and age data of the A'nyemaqen ophiolites, and combined with the stratigrphical relationship of Majixueshan mafic rocks and Carboniferous and Permian strata as well as the contained Carboniferous and Permian limestone blocks inside the mafic rocks[14], it can be inferred that the age of the Majixueshan ophiolites probably is identical to the ages of both the Dur'ngoi and Buqingshan ophiolites.

2 Samples and analysis methods

Twenty one samples in this study were taken from Buqingshan, Dur'ngoi and Majixueshan ophiolites, respectively. 9 Buqingshan samples are all pillow lava and from the area to west of the Delisitan valley, located on the outcrop of the late-Paleozoic ophiolites (OM2) determined by Bian et al.[11]. Of 7 Dur'ngoi samples, 3 were collected from the Dur'ngoi valley and the others from the tectonic blocks of ultramafic-mafic rocks

mixed with Carboniferous carbonaceous slates in an about 60-m-long outcrop in adjacent Maqin-Gande highway. 5 Majixueshan basaltic samples were taken from the Qianliwalima area to southwest of the Majixueshan Mountain.

To ensure no metasomatic effect on the samples, before crushing, all the samples were carefully selected by eliminating episode and carbonate veins and weathered parts. The major and trace element analyses were performed in National Key Lab of Continental Dynamics, Northwest University. In the major element assay, wet chemistry method was used in analysis of LOI, the other major elements were measured by XRF (RIX2100X X-ray fluorescence). A within 5% error was achieved by multiple measurements of standards BCR-2 and GBW07105. Trace elements, including REE were analyzed by ICP-MS (Elan 6100DRC) and the analysis procedure following the technique described by Runick et al.[17]. Analysis errors for Rb, Y, Zr, Nb, Hf, Ta and LREE were smaller than 5% and 5%—15% for the others.

3 Geochemistry

From the regional geology described above, it is known that the ophiolites in the A'nyemaqen ophiolite zone are commonly subjected to greenschist facies metamorphism. Metamorphic effects on reliability of trace elements used to discuss compositions of primary rocks have been debating all the time. Based on Granch's study[18], the REE patterns of various metamorphic rocks under different physico-chemical conditions are consistent with the patterns of those unmetamorphic rocks, basically ruling out metamorphic influence on REE geochemistry. For HFSE such as Zr, Hf, Nb, Ta and P, their immobility during metamorphic processes has been recognized by geological studies. As to mobility of U, Th and Pb, Moorbath et al. argued that they show strong mobility only in high-grade metamorphism[19]. Hence, using them to discuss geochemistry of the primary rocks undergoing greenschist metamorphism in this area can be safe and reliable. In fact, the previous studies on geochemistry, tectonic discrimination and geochronology (Ar/Ar method) of the ophiolites have proved that the metamorphic effects are limited[11,13,15].

3.1 Major elements geochemistry

Major element analyses are presented in Table 1. As shown in Table 1, the $Mg^{\#}$ values (Mg/(Mg+Fe) × 100) of all the mafic samples (no matter identified as OIB or MORB-see below) range from 57 to 67, of which, the Majixueshan samples are 60—65, Buqingshan samples 54—67 and Dur'ngoi samples 57—67. The $Mg^{\#}$ values of the mafic rocks from the different ophiolites overlap one another and exhibit little difference. These values indicate that the primary magma of the mafic rocks experienced differentiation to some degree. SiO_2 for the samples is 43.58%—51.75%, Na_2O+K_2O is 2.2%—5.46%. Most samples are discriminated as subalkaline series basalts using the TAS (Na_2O+K_2O-SiO_2) diagram.

3.2 REE and race element geochemistry

Trace elements and REE analyses and relevant ratios are listed in Table 1.

All basaltic samples are plotted on 2Nb-Zr4-Y diagram (Figure 2), 4 Dur'ngoi samples (AM-1, AM-2, AM-3 and AM-4) fall in AI+AII area, 1 Buqingshan and 5 Majixueshan samples also fall in the same area, reflecting that they are within-plate originated basalts. 3 Dur'ngoi samples and 8 Buqingshan samples belong to N-MORB as plotted in the D area.

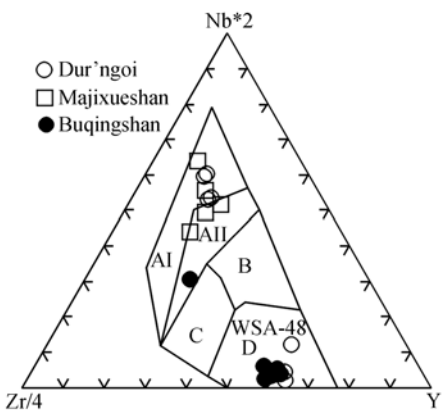

Figure 2 2Nb-Zr4-Y diagram of mafic rocks from different ophiolites in the A'nyemaqen ophiolite zone (from Meschede[20]). A, WPA, WPT; B, P-type MORB; C, VAB; D, N-type MORB.

For clearness, the Majixueshan within-plate basaltic samples will be separated from the other samples of both the Dur'ngoi and Buqingshan ophiolites in the following description.

The Dur'ngoi and Buqingshan samples plotted in the within-plate area in Figure 2 show enrichment in LREE and depletion in HREE and right-dip REE patterns on the chondrite-normalized REE distribution diagram (Figure 3). They have $(Sm/La)_N$ = 0.3, $(La/Yb)_N$ = 5—10,

Table 1 Major and trace element analyses of mafic rocks (major elements: %; trace elements: $\mu g \cdot g^{-1}$)

Area	Dur'ngoi							Majixueshan			
Sample &	WSA-47	WSA-47-1	WSA-48	AM-1	AM-2	AM-3	AM-4	MJX-5	MJX-8	MJX-11	MJX-18
rock type	NMORB	NMORB	EMORB	OIB	OIB	OIB	OIB	OIB	OIB	OIB	OIB
SiO_2	50.10	51.07	49.07	43.99	44.65	45.25	45.15	49.45	43.58	45.8	48.53
TiO_2	1.28	1.26	1.46	1.99	2.08	2.33	2.12	0.83	2.38	1.65	1.02
Al_2O_3	14.07	15.04	13.06	16.68	15.31	16.94	16.96	13.85	12.88	12.94	13.55
TFe_2O_3	9.87	9.85	16.20	11.92	12.63	10.17	11.63	10.75	12.91	13.26	12.27
MnO	0.16	0.18	0.21	0.30	0.18	0.35	0.36	0.17	0.2	0.22	0.18
MgO	7.75	7.79	6.32	6.98	9.37	6.53	6.09	8.19	11.93	11.08	9.97
CaO	11.07	10.04	9.33	7.83	7.11	8.96	8.20	11.23	11.25	9.76	8.7
Na_2O	2.66	2.64	2.89	3.25	2.30	2.60	3.48	2.63	1.82	2.34	2.71
K_2O	0.03	0.02	0.35	0.99	1.23	2.13	1.03	0.11	0.38	0.24	0.24
P_2O_5	0.11	0.23	0.12	0.45	0.36	0.55	0.51	0.08	0.53	0.51	0.08
LOI	2.52	2.41	0.83	5.13	4.40	3.72	4.01	2.21	1.79	1.98	2.92
Total	99.62	100.53	99.81	99.51	99.60	99.53	99.54	99.5	99.65	99.76	100..2
$Mg^{\#}$	66	67	53	60	66	62	57	60	64	63	62
Rb	0.152	0.146	14.41	25.99	26.87	55.5	24.44	5.34	4.26	3.51	6.5
Sr	105.3	105.1	133	357	201	212	340	234	327.15	174.32	324
Y	34.6	34.5	39.0	29.0	25.9	30.6	33.3	28.8	26.92	33.09	31.2
Zr	80.5	79.5	73.9	189	155	180	235	174	242.53	149.70	239
Nb	0.92	0.92	4.02	58.1	36.6	42.1	68.0	35.3	77.23	37.77	35.6
Cs	0.013	0.014	0.403	1.85	0.606	1.31	0.843	0.440	0.30	0.28	0.76
Ba	7.60	7.51	100.3	827	555.8	610.1	438.9	484.3	393.16	261.16	267.8
La	2.23	2.26	3.90	38.0	25.7	34.0	42.0	30.6	54.86	119.06	31.8
Ce	8.00	8.11	9.64	70.3	51.8	67.9	81.4	78.7	110.68	208.57	64.3
Pr	1.41	1.43	1.42	7.61	5.97	7.87	9.11	10.03	12.64	20.93	8.71
Nd	8.96	8.94	8.03	31.7	26.4	34.3	37.7	38.9	46.58	66.67	44.4
Sm	3.40	3.38	2.96	6.24	5.70	7.09	7.52	6.47	8.64	10.71	7.35
Eu	1.25	1.24	1.07	2.02	1.84	2.29	2.38	2.14	2.70	3.25	1.98
Gd	4.10	4.09	3.87	6.13	5.51	6.86	7.18	5.88	6.77	8.39	7.64
Tb	0.83	0.83	0.84	0.89	0.85	1.01	1.05	1.21	1.04	1.30	0.97
Dy	5.42	5.40	5.85	4.92	4.68	5.51	5.78	4.78	5.21	6.63	5.09
Ho	1.23	1.24	1.41	1.01	0.93	1.09	1.16	1.08	0.94	1.25	1.11
Er	3.22	3.22	3.91	2.61	2.36	2.73	3.04	2.43	2.34	3.24	2.74
Tm	0.51	0.51	0.65	0.39	0.35	0.40	0.46	0.47	0.30	0.45	0.44
Yb	3.36	3.36	4.52	2.54	2.24	2.51	2.99	2.28	1.88	2.89	2.65
Lu	0.53	0.53	0.74	0.41	0.35	0.39	0.47	0.36	0.27	0.44	0.45
Hf	2.36	2.33	2.21	4.07	3.79	4.28	5.26	3.81	4.76	3.40	5.24
Ta	0.11	0.11	0.31	3.51	2.22	2.55	4.06	2.23	4.28	2.02	2.88
Pb	0.758	0.612	0.593	5.16	1.81	3.21	3.70	2.87	4.69	3.02	5.79
Th	0.087	0.086	0.54	6.53	3.19	4.05	6.32	3.77	6.30	17.42	1.39
U	0.043	0.042	0.134	1.44	0.73	1.43	1.27	1.73	1.72	4.64	1.68
Nb/U	21.40	21.76	29.97	40.21	50.01	29.38	53.54	20.40	44.90	8.10	21.20
Ce/Pb	10.55	13.25	16.26	13.61	28.54	21.13	22.01	27.40	23.60	69.10	11.12
Zr/Nb	87.43	86.70	18.39	3.26	4.23	4.27	3.45	4.93	3.14	3.96	6.70
Ba/La	3.40	29.05	25.72	21.79	21.61	17.96	10.45	15.80	7.17	2.19	8.42
La/Nb	2.43	2.46	0.97	0.65	0.70	0.81	0.62	0.87	0.71	3.15	0.89
Ba/Nb	8.26	8.19	24.96	14.25	15.18	14.50	6.45	13.70	5.09	6.91	7.52
$(Sm/La)_N$	2.24	2.38	1.20	0.26	0.35	0.33	0.28	0.33	0.24	0.14	0.37
$(Sm/Yb)_N$	1.09	1.08	0.70	2.64	2.73	3.03	2.70	3.04	4.94	3.98	2.98
$(La/Yb)_N$	0.45	0.45	0.58	10.11	7.75	9.15	9.49	9.07	19.71	27.83	8.11

(*To be continued on the next page*)

(*Continued*)

Area	Majixueshan	Buqingshan								
Sample & rock type	MJX-20 OIB	AMH-1 OIB	BQ5 NMORB	BQ6 NMORB	BQ7 NMORB	BQ8 NMORB	BQ9 NMORB	BQ10 NMORB	BQ11 NMORB	BQ12 NMORB
SiO_2	50.55	51.24	46.65	45.27	46.67	50.28	47.59	49.30	48.48	47.59
TiO_2	0.77	3.23	1.43	1.34	1.58	1.44	1.38	1.42	1.44	1.32
Al_2O_3	13.75	13.18	15.86	15.15	17.18	15.70	16.00	15.76	15.75	15.60
TFe_2O_3	11.06	12.36	10.88	10.32	11.94	10.80	10.62	11.08	10.57	10.57
MnO	0.18	0.16	0.16	0.17	0.15	0.15	0.12	0.17	0.16	0.15
MgO	8.8	6.78	8.21	7.19	9.19	6.49	6.42	6.93	8.67	6.89
CaO	8.81	6.05	7.92	12.29	3.85	6.88	6.97	7.39	7.48	7.85
Na_2O	3.5	3.25	4.06	3.23	5.01	5.42	4.94	4.92	4.28	5.13
K_2O	0.16	0.71	0.05	0.03	0.07	0.06	0.04	0.31	0.06	0.05
P_2O_5	0.07	0.52	0.11	0.11	0.10	0.11	0.11	0.12	0.11	0.11
LOI	2.39	2.94	4.79	4.46	4.65	3.04	6.23	2.91	3.45	4.45
Total	100.04	100.42	100.12	99.56	100.39	100.37	100.42	100.31	100.45	99.71
Mg#	61	60	65	57	61	60	54	56	67	56
Rb	3.19	10.41	1.13	0.67	1.80	1.62	1.11	9.68	1.42	1.21
Sr	284.62	148	176	184	103.9	225	240	160	261	242
Y	27.80	53.7	37.3	37.3	36.1	37.1	35.6	38.1	37.2	35.8
Zr	178.00	365	89.5	87.6	94.3	90.1	85.7	89.2	89.6	84.4
Nb	45.25	32.1	1.24	1.29	1.31	1.24	1.16	1.72	1.23	1.14
Cs	0.53	0.535	0.656	0.216	0.420	0.856	0.201	0.91	0.134	0.199
Ba	545.78	194.2	31.94	34.11	25.61	72.52	30.62	59.70	35.79	30.33
La	44.90	26.3	2.35	2.38	2.28	2.11	2.29	2.51	2.31	2.29
Ce	78.46	59.6	8.30	8.33	8.71	7.56	8.02	8.33	8.26	7.98
Pr	10.34	7.97	1.49	1.49	1.50	1.38	1.43	1.45	1.47	1.42
Nd	35.67	38.5	9.04	8.98	9.09	8.57	8.67	8.76	9.03	8.67
Sm	8.39	10.2	3.38	3.31	3.47	3.27	3.19	3.29	3.33	3.21
Eu	2.39	3.02	1.14	1.15	1.01	1.07	1.12	1.15	1.07	1.10
Gd	6.69	10.12	4.05	4.00	4.15	3.89	3.90	3.97	4.02	3.78
Tb	1.08	1.68	0.84	0.82	0.85	0.82	0.79	0.83	0.82	0.77
Dy	5.54	9.1	5.43	5.35	5.61	5.39	5.24	5.38	5.34	5.02
Ho	1.10	1.74	1.21	1.18	1.24	1.19	1.16	1.21	1.20	1.11
Er	2.14	4.14	3.19	3.18	3.28	3.21	3.02	3.18	3.14	2.91
Tm	0.34	0.59	0.52	0.52	0.53	0.51	0.49	0.52	0.50	0.46
Yb	2.29	3.74	3.50	3.39	3.52	3.46	3.26	3.48	3.31	3.12
Lu	0.37	0.56	0.57	0.54	0.55	0.55	0.52	0.54	0.53	0.48
Hf	4.35	7.88	2.47	2.32	2.59	2.46	2.30	2.41	2.39	2.19
Ta	2.34	1.98	0.10	0.11	0.10	0.11	0.10	0.13	0.10	0.09
Pb	3.15	1.15	0.700	0.89	0.550	0.758	0.95	0.824	0.601	0.91
Th	6.18	2.86	0.102	0.125	0.092	0.110	0.075	0.213	0.092	0.075
U	1.45	0.88	0.074	0.061	0.150	0.205	0.058	0.098	0.045	0.059
Nb/U	29.30	36.51	16.75	21.17	8.73	6.07	20.11	17.47	27.32	19.48
Ce/Pb	24.91	51.90	11.86	9.40	15.84	9.97	8.41	10.11	13.75	8.82
Zr/Nb	3.93	11.37	72.41	67.70	71.76	72.38	73.89	51.92	72.90	73.86
Ba/La	12.16	7.37	13.61	14.34	11.25	34.43	13.35	23.79	15.51	13.25
La/Nb	0.99	0.82	1.90	1.84	1.73	1.69	1.98	1.46	1.88	2.00
Ba/Nb	12.06	6.04	25.84	26.37	19.50	58.27	26.41	34.73	29.13	26.53
$(Sm/La)_N$	0.30	0.62	2.29	2.21	2.42	2.46	2.21	2.08	2.29	2.23
$(Sm/Yb)_N$	3.93	2.93	1.04	1.05	1.06	1.01	1.05	1.01	1.08	1.10
$(La/Yb)_N$	13.25	4.75	0.45	1.05	0.44	0.41	0.47	0.49	0.47	0.50

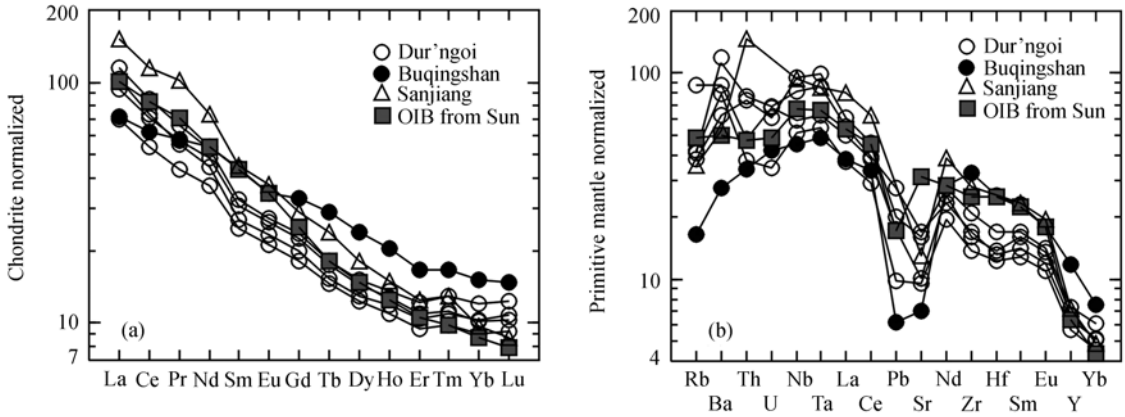

Figure 3 (a) Chondrite-normalized REE concentration patterns of the Dur'ngoi and Buqingshan within-plate basaltic rocks; (b) primitive-mantle-normalized concentration patterns of incompatible elements in the Dur'ngoi and Buqingshan within-plate basaltic rocks (the normalizing value and data of the typical OIB from Sun et al.[21], Sanjiang OIB from Hou et al.[7]).

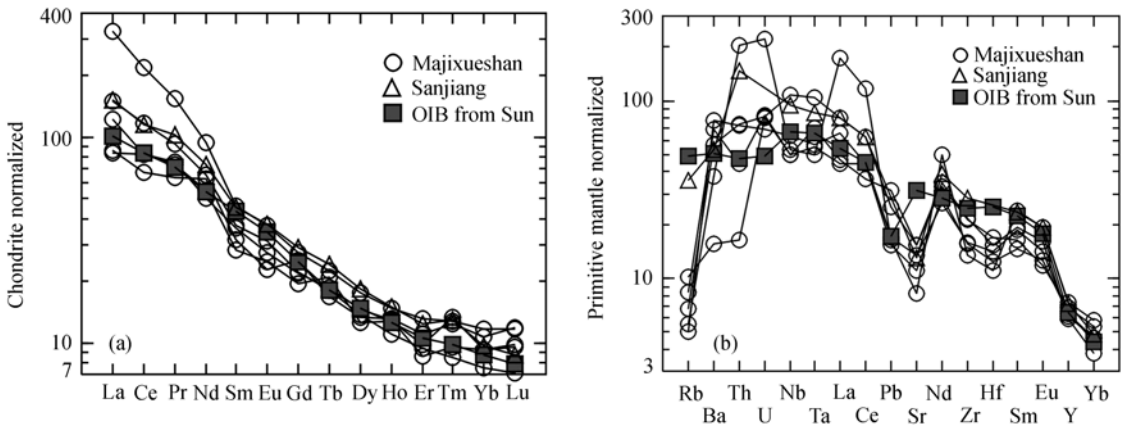

Figure 4 (a) Chondrite-normalized REE concentration patterns of the Majixueshan within-plate basaltic rocks (b) primitive-mantle-normalized concentration patterns of incompatible elements in the Majixueshan within-plate basaltic rocks (the normalizing value and data of the typical OIB from Sun et al.[21], Sanjiang OIB from Hou et al.).

and high ΣREE, identical to the OIB REE pattern of Sun et al. and thus, possess OIB property. Compared with the contemporaneous OIB in the Sanjiang region, they have the similar pattern.

The primitive-mantle-normalized concentration patterns of incompatible elements for the above samples exhibit enrichment in incompatible elements (Figure 3(a)), identical to the typical OIB. But, the samples commonly have Sr depletion, 2 samples (AMH-1 and AM-2) from Dur'ngoi and Buqingshan possess strong Pb depletion. The Sr depletion of the rocks probably reflects fractional crystallization of plagioclase from the primary magma.

The REE patterns of 5 Majixueshan samples (Figure 4(a)) display the similarity to the OIB in Dur'ngoi and Buqingshan (Figure 3(a)), their $(La/Yb)_N > 5$ and sample MJX-11 shows a strong LREE-HREE fractionation. In comparison with the typical OIB of Sun et al. and the OIB from the Sanjiang region, most samples have the similar REE patterns, with exception of MJX-11 that has a steeper LREE pattern, and obviously exhibit OIB characteristics. The primitive-mantle-normalized concentration patterns of the samples (Figure 4(b)) resemble the typical OIB, featured enrichment in incompatible elements. Similar to the samples from Dur'ngoi and Buqingshan, the Majisueshan samples also show the moderate Sr depletion.

The samples (from the Dur'ngoi and Buqingshan ophiolites) discriminated as N-MORB on the 2Nb-Zr4-Y diagram have the typical REE patterns of the rock type. They show left-dip REE patterns with flat HREE and strong depletion in LREE (Figure 5(a)), most samples have $(Sm/La)_N > 2$ and $(La/Yb)_N = 0.41—0.5$. Compared with the same type of rocks from Sanjiang region and

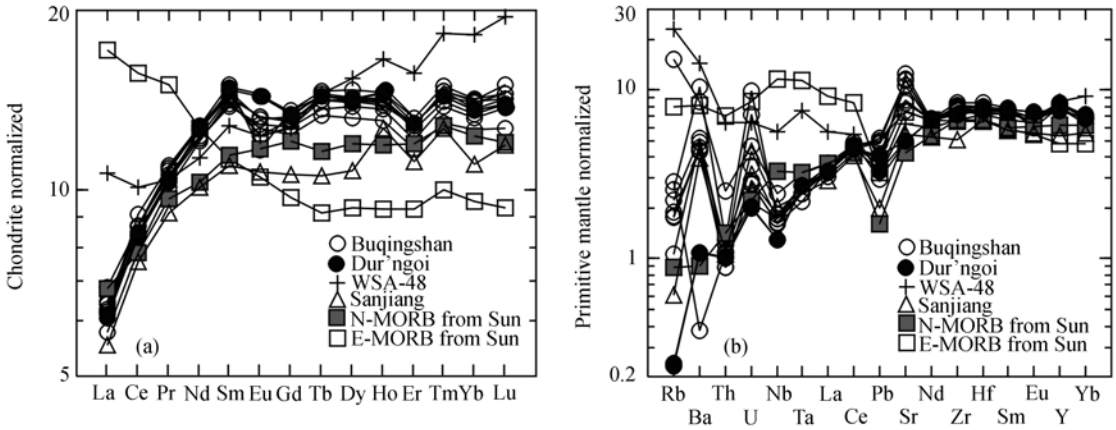

Figure 5 (a) Chondrite-normalized REE concentration patterns of the MORB from Dur'ngoi and Buqingshan; (b) primitive-mantle-normalized concentration patterns of incompatible elements in the MORB from Dur'ngoi and Buqingshan (the normalizing value of primitive mantle and data of the typical N-MORB and E-MORB from Sun et al.[21], Sanjiang N-MORB from Xu et al.[9]).

Sun et al. the rocks in the study area show higher ΣREE. As noted in Figure 5(a), the sample WSA-48 is different from most samples and characterized by a gentle left-dip curve and higher ΣREE.

On the diagram of Primitive-mantle-normalized concentration patterns of incompatible elements (Figure 5(b)), the N-MORB samples from the study area exhibit depletion in incompatible elements, identical to the patterns of the typical N-MORB, with exception of Sr depletion. It is noted that sample WSA-48 displaying a N-MORB pattern in Figure 5(a), shows the similarity of E-MORB in Figure 5(b). Hence, WSA-48 probably belongs to E-MORB rather than N-MORB. This judgment seems against the discrimination on the 2Nb-Zr4-Y diagram (Figure 2) where WSA-48 falls in the D area (N-MORB area). However, it can be seen that on the 2Nb-Zr4-Y diagram, the plot of WSA-48 is close to the B area (enriched), showing an affinity of E-MORB.

It has been thought that Nb/U and Ce/Pb ratios are effective and sensitive tracers in study of oceanic basalts (including both MORB and OIB) and compositions of their source region[22−25]. The Nb/U ratios of OIB in the study area have a range of 8—50, most samples have smaller ratios relative to Hafmann's ratio (47) for OIB and to the ratio (43) of the Kerguelen OIB of a ridge-centered hotspot from the southern Indian Ocean[21,24]. For the Ce/Pb ratio, except the sample AMH-1 having 52, the ratios of most samples range from 11 to 28 that are higher than the ratio of 15 from Kerguelen OIB[21], but still lower than the ratio of 25 given by Hafmann[24].

The Nb/U and Ce/Pb ratios of 10 N-MORB samples are 6—30 (most are around 20) and 11—16, respectively. These ratios are lower than the ratios (Nb/U=50 and Ce/Pb=25) given by Sun et al. and those (Nb/U=40—50 and Ce/Pb=19—23) of N-MORB from Central Indian and Carlsburg Ridge in the Indian Ocean[21,23]. Only one E-MORB sample WSA-48 has Nb/U=30 and Ce/Pb =16, lower than the typical E-MORB (46, 25)[21].

In general, the basaltic rocks of the study area are featured by lower NB/U and Ce/Pb ratios, compared with the same type of oceanic basalts in the world.

The Nb/U and Ce/Pb ratios of N-MORB in the Shuanggou area in the Sanjiang region reported by Xu et al.[9] are used to carry out the comparison with the local rocks. The results indicate that the N-MORB from the study area are similar to the Shuanggou N-MORB (17 on average) in Nb/U and lower than the Shuanggou (20 on average) in Ce/Pb. Due to lack of OIB ratios in the Sanjiang region, the comparison for OIB cannot be implemented.

4 Discussion: Majixueshan ridge-centered hotspot

The above lithological geochemistry demonstrates that the association of N-MORB, E-MORB and OIB is a major part of the A'nyemaqen ophiolite zone. The association, at first, represents the remains of the A'nyemaqen oceanic basin as a branch of the paleo-Tethyan Ocean basin, and more important, their spatial configuration in

the study area reveals a tectonic environment of the Iceland-like ridge-centered hotspot.

4.1 Significance of lithological association and spatial distribution

As the eastern portion of the A'nyemaqen ophiolite zone, the Dur'ngoi ophiolites hava the association of N-MORB, OIB and E-MORB, while in the middle portion, the Majixueshan mafic rocks consist mainly of OIB. In the western portion, the Buqingshan ophiolites, only one sample of OIB was found in the study. However, according to Bian et al., some T-MORB have been identified in the Buqingshan area[11]. Also, Hou et al. reported finding of P-MORB in the same area[26]. Moreover, we have noticed that besides the recognized T-MORB in the late Paleozoic basalts, a few samples (e.g., DL99-51) with enrichment in Pb and depletion in Nb probably are of E-MORB. So, similar to the Dur'ngoi ophiolites, the Buqingshan also exhibits the association of N-MORB, OIB and E-MORB.

From the rock types in the above three ophiolite occurrences, it can be obviously seen that the mafic rocks of the A'nyemaqen ophiolite zone make up a transitional change pattern in east-west direction around the Majixueshan. To the west from the Majixueshan OIB, the rocks become N-MORB plus OIB and E-MORB in the Buqingshan ophiolites, while to the east they change into the N-MORB, OIB and E-MORB association in the Dur'ngoi area (Figure 6). This spatial distribution pattern of mafic rock types is comparable with the Iceland hotspot. It appears that the Majisueshan OIB occupies the central location of the hotspot, that is the site of the ocean island. The distribution of volcanic rocks in Iceland is featured by the central OIB in island itself and the N-MORB in the surrounding areas especially along the axis of the mid-ocean ridge[27,28]. The hotspot in Iceland reflects the mantle plume activities under the island[27−30] and as a result of the superposition of the rising plume on the mid-ocean ridge, the on-ridge island was formed[28]. In addition, the chemical interaction and mixture between the materials from the distinctive sources resulted in generation of different types of basalts[27,31] that are distributed around the hotspot in space.

In the Iceland hotspot, not only the compositional anomalies and the characteristic distribution of the mafic rock types along the ridge, but also the thickened crust and corresponding changes of geophysical field in the expression of topographic rise can be observed[1]. Compared with the modern Iceland hotspot, the corresponding geomorphological and geophysical features cannot be seen in the paleo-Majixueshan hotspot situated in the ophiolite zone. However, the basaltic lava and gabbros in thickness greater than a few thousand meters, probably are the remains of the Majixueshan ocean island formed above the mid-ocean ridge. Due to its great crustal thickness, it is relatively hard for the Majixueshan ocean island to subduct and is finally preserved in the ophiolites.

4.2 Relationship of MORB and OIB

If given rock association and spatial distribution are taken into account, then these phenomena in the

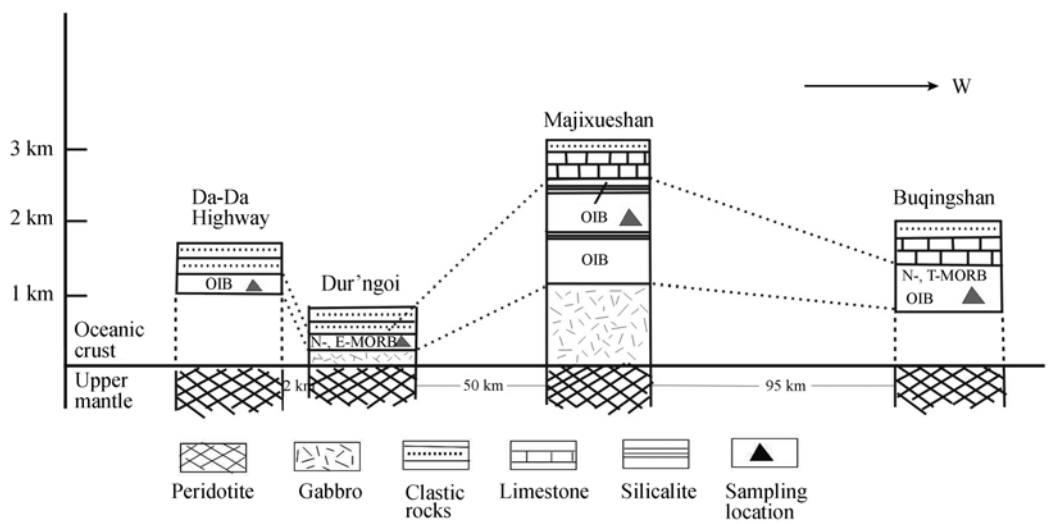

Figure 6 Distribution of different mafic rocks surrounding the Majixueshan in the A'nyemaqen ophiolite zone (For thickness of the strata refer to refs. [11,13,14]).

A'nyemaqen ophiolites could also be observed in an ocean island and its surrounding MORB crust. However, it should be emphasized that the transitional change of rock types around the Majixueshan reflects a metasomatic link existing between the plume materials and the upper mantle MORB source, and it is because of this geochemical genesis relationship that the characteristic rock association and distribution have occurred.

The geochemical results indicate that relative to the same type rocks in the world, the Nb/U and Ce/Pb ratios of OIB in the study area vary in a wide range and are low as a whole. The low Nb/U and Ce/Pb ratios in the EM-type OIB are sensitive indicators of crustal contamination[23]. Combined with the great range of trace element contents in the OIB, of which some are depleted in Nb and Sr, it can be inferred that the OIB source could contain input derived from the continental crust in the subducted oceanic sediments and belong to the EM-type[5,24,32]. Moreover, the N-MORB of the study area have low and scattered Nb/U and Ce/Pb ratios and the similar ratios (Nb/U = 22, Ce/Pb = 15) have been recently obtained from the Zongwulong tectonic belt between the Qilian orogen and the northern Qaidam tectonic belt (will be discussed elsewhere), and these ratios are identical to those in the OIB. Thus, the low Nb/U and Ce/Pb ratios seem to be the common characteristics in the Paleozoic oceanic basalts in this region. In study of Nb/U and Ce/Pb ratios of MORB and OIB, Hafmann pointed out that they are excellent tracers of continental components in OIB and the similar values present in MORB and OIB indicate their genetic link[33]. Rehkamper et al. suggested that low Nb/U and Ce/Pb ratios and high $^{87}Sr/^{86}Sr$ ratios in the Central Indian and Carlsburg Ridge in the Indian Ocean characterize the enriched end member that results in crustal contamination in the upper mantle MORB source region[23,28]. Based on the similar Nb/U and Ce/Pb ratios in the local OIB and MORB and their field relationship (see below), the enriched end member could be the OIB, while the MORB source region was more or less metasomatized by OIB composition from the EM-type source region and generated the E-MORB and N-MORB with the above-mentioned geochemistry. The Nb/U and Ce/Pb ratios lower than the typical OIB and MORB possibly imply more continental input contained in the OIB source in this region.

On the basis of Sr and Pb isotopic composition, Bian et al. interpreted that the magamtic source of the basalts in this region could be a mixed one between the DMM and EMII[11]. From their data, the $^{87}Sr/^{86}Sr$ ratios (0.7054—0.7081) of the Paleozoic MORB in the Buqingshan ophilites are far greater than those from the MORB in the Indian Ocean (0.7025—0.7031)[23], and the $^{206}Pb/^{204}Pb$ ratios are similar to those from the inferred Indian Ocean plume ($^{206}Pb/^{204}Pb \geqslant 18$). The isotope data with the Nb/U and Ce/Pb ratios from this study identically offer the information of the contaminated mantle source by the continental components in the form of the EMII. It also demonstrates that in addition to the Sr and Pb isotopes, the Nb/U and Ce/Pb ratios can be quite useful in determining contamination of a magmatic source region. Although Bian et al. did not find the OIB and discuss the relationship with EMII component, by the consideration of the similarity of the Nb/U and Ce/Pb ratios in both OIB and MORB and their relationship in the field, we infer that the OIB in the study area probably is the EMII end member equivalent (has to be further proved by isotope study). The previously reported P-MORB and T-MORB, and the E-MORB found in this study could all be products of mixed DMM and EMII, whereas the Sr and Pb isotopic geochemistry and the Nb/U and Ce/Pb ratios in the N-MORB indicate the presence of the mixture and metasomatism.

The thoughts for existence of the OIB equivalent EM-type source and the metasomatic MORB source in this region are also supported by the following arguments in a broad sense[23,24]: (i) the paleo-Tethyan Ocean and the present-day Indian Ocean are spatially comparable and they share the same oceanic basaltic source region having the Dupal anomaly[9]; (ii) the EM-type source region only exists in the Indian Ocean-centered southern hemisphere; and (iii) the MORB source region of Indian Ocean contains some pelagic sediments. Upwelling of the plume materials derived from the EM-type source represented by OIB and interaction with the MORB source in the depleted upper mantle by metasomatism finally generated the Iceland-like rock assemblage in the certain spatial distribution.

The metasomatism is generally thought to occur in the asthenosphere, that is the MORB source region. The plume bringing the EM-type materials meatsomatizes the upper mantle on the way up along the certain channels at the base of lithosphere and formed various incompatible elements enriched MORB source regions[4,28].

From the field occurrence, it is evident for the OIB materials metasomatizing the MORB materials. On an outcrop scale, there is no clear-cut limit in terms of structure and lithology for the N-MORB, OIB and E-MORB, different rock types can either be exposed on the different outcrops or occur on the same outcrop (the latter such as WSA-48 and WSA-47, AMH-1 and BQ-5). In this case, the tectonic mixing cannot be ruled out as a cause for different rock types on the different exposures (even so, the tectonic mixing is still on a small scale for the rock blocks having some genetic link, according to their geochemical characteristics). On the other hand, the different rock types on the same exposure demonstrate that the source region could have experienced heterogeneous metasomatism. On the scale of the entire ophiolite zone, the above-discussed rock assemblages in the different ophiolite occurrences and the transitional relationship with the Majixueshan OIB are hardly observed in an ocean island and its surrounding oceanic crust. Although the latter could have the same configuration in space, it exhibits a non-transitional relationship on outcrops on different scales without metasomatism in their origin.

4.3 In comparison with Sanjiang region

In the above comparison, it can be seen that the OIB and MORB in the area have the similar geochemistry to the same rocks in the Sanjiang region. The N-MORB can be compared with the Shuanggou MORB in the Sanjiang region in the Nb/U and Ce/Pb ratios. The similarities of the Paleozoic oceanic crust in both the Sanjiang region and the study area could have had the same magmatic origin, including the N-MORB source from the depleted upper mantle and the plume represented by the OIB as well as the latter metasomatizing the former[7]. The low Nb/U and Ce/Pb ratios in the two areas commonly reflect the influence on the source region of the paleo-Tethys Oceanic crust by the EM components. The presence of E-MORB in the Jinshajiang area and the Indian Ocean-affinity MORB can be evidence for this[9].

After the A'nyemaqen ophiolite zone was formed in the Indosinian period, it was subjected to deformational reworking during the Mesozoic-Cenozoic intracontinental orogeny, which could result in the integration of different tectonic blocks in the zone. However, it is noteworthy to mention that after the Indosinian amalgamation of China's continent, the later intracontinental orogeny was mainly in the fashion of extensional collapse, strike-slip of fault blocks and thrust and nappe[10]. From present studies, as the major suture between the Yangtze plate and the east Kunlun-west Qinling orogen during the Indosinian amalgamation of China's continent, the A'nyemaqen ophiolite mélange has been mainly involved in the east-west oriented strike-slip movement during the Mesozoic-Cenozoic intracontinental orogeny, and no large-scale tectonic disturbances. In addition, based on Xu et al., since the Indosinian the strike-slip faults have been formed on both sides of the ophiolite zone[34]. In another word, the original structures and textures of the A'nyemaqen ophiolite zone formed in the final Indosinian collision have been kept.

Finding of the Majixueshan ridge-centered hotspot and presence of the Sanjiang paleo-Tethyan mantle plume[6,7] as well as N-MORB, E-MORB and OIB reported in the Qinling orogen[8,35−37] all indicate that the hotspot could be a main cause for the Paleozoic extensional environment (e.g., continental rift and ocean-continent triple-junction). If the vertical mantle plume dynamically played a major role in the open-up of the paleo-Tethyan ocean, and the horizontal plate tectonics could have been the secondary driving force for the formation of the numerous ocean basins. The combination of both vertical plume and the horizontal plate tectonics and their interaction as well eventually forged China's continent characterized by multi-block tectonics and the Indosinian amalgamation. Therefore, in order to obtain a complete picture of continental dynamics in the paleo-Tethyan study, exploring the combining mechanism of the plume and plate tectonics would be a necessary approach.

Thanks to the anonymous referees for their valuable comments and constructive suggestions.

1 Ito G, Lin J, Gable C W. Dynamics of mantle flow and melting at a ridge-centered hotspot: Iceland and the Mid-Atlantic Ridge. Earth Planet Sci Lett, 1996, 144: 53−74[DOI]
2 Mattieli N, Weis D, Gregoire M, et al. Evidence for long-lived Kerguelen hotspot activity. Lithos, 1996, 37: 261−280[DOI]
3 Galdcezenko T P, Coffin M F, Eldholm O. Crustal structure of the Ontong Java Plateau: modeling of new gravity and existing seismic data. J Geophys Res, 1997, 102/B10: 22711−22729[DOI]
4 Storey M, Pedersen A K, Stecher O, et al. Long-lived postbreakup magmatism along the East Greenland margin: Evidence for shallow-mantle metasomatism by the Iceland plume. Geol Soc Am, 2004, 2: 173−176[DOI]

5 Eisele J, Sharma M, Galer S, et al. The role of sediment recycling in EM-1 inferred from Os, Pb, Hf, Nd, Sr isotope and trace element systematics of the Pitcairn hotspot. Earth Planet Sci Lett, 2002, 196: 197－212[DOI]

6 Hou Z Q, Mo X X, Zhu X W, et al. Mantle plume in the Sanjiang paleo-Tethyan region, China: evidence from ocean-island basalts. Acta Geosci Sin (in Chinese), 1996, 17: 343－361

7 Hou Z Q, Mo X X, Zhu X W, et al. Mantle plume in the Sanjiang paleo-Tethyan lithosphere:evidence from mid-ocean ridge basalts. Acta Geosci Sin (in Chinese), 1996, 17: 362－375

8 Zhang B R. Magmatic activitiesfrom plume-source in the Qinling belt and its dynamic significance. Earth Sci Front (in Chinese), 2001, 8: 57－66

9 Xu J F, Castillo P R. Geochemical and Nd-Pb isotopic characteristics of the Tethyan asthenosphere: implications for the origin of the Indian Ocean. Tectonophysics, 2004, 393: 9－27[DOI]

10 Zhang G W, Dong Y P, Lai S C, et al. Mianlue tectonic zone and Mianlue suture zone on southern margin of Qinling-Dabie orogenic belt, Sci China Ser D-Earth Sci, 2004, 47(4): 300－316

11 Bian Q T, Li D H, Pospelov I, et al. Age, geochemistry and tectonic setting of Buqingshan ophiolites, North Qinghai-Tibet Plateau, China. J Asian Earth Sci, 2004, 23: 577－596[DOI]

12 Chen L, Sun Y, Liu X M, et al. Geochemistry of Dur'ngoi ophiolite and its tectonic significance. Acta Petrol Sin (in Chinese), 2000, 16(1): 106－110

13 Yang J X, Wang X B, Shi R D, et al. The Dur'ngoi ophiolite in east Kunlun, northern Qinghai-Tibet Plateau: a fragment of paleo-Tethyan oceanic crust. Geol Chin (in Chinese), 2004, 31(3): 225－239

14 Jiang C F, Yang J S, Feng B G, et al. Opening-Closing Tectonics of the Kunlun Mountains (in Chinese). Beijing: Geological Publishing House, 1992. 188

15 Chen L, Sun Y, Pei X Z, et al. Northernmost paleo-Tethyan oceanic basin in Tibet: Geochronological evidence from $^{40}Ar/^{39}Ar$ age dating of Derni ophiolite. Chin Sci Bull, 2001, 46(14): 424－426

16 Zhang K X, Lin Q X, Zhu Y H, et al. New paleontological evidence on time determination of the east part of the Eastern Kunlun Mélange and its tectonic significance. Sci Chin Ser D-Earth Sci, 2004, 47(2): 857－865

17 Runick R, Gao S, Ling W L, et al. Petrology and geochemistry of spinel peridotite xenoliths from Hannuoba and Qixia, North China craton. Lithos, 2004, 77: 609－637[DOI]

18 Grauch R I. Rare earth elements in metamorphic rocks. In: Lipin B R, McKay G A, eds. Geochemistry and Mineralogy of Rare Earth Elements, Reviews in Mineralogy Vol.21. Washington, D.C: Mineralogical Society of America, 1989, 147－167

19 Moorbath S, Welke H, Gale N H. The significance of lead isotope studies in ancient high-grade metamorphic basement complexes, as exemplified by the Lewisian rocks of northwest Scotland. Earth Planet Sci Lett, 1969, 6: 245－256

20 Meschede M A. A method of discriminating between different types of mid-ocean ridge basalts and continental tholeiites with the Nb-Zr-Y diagram. Chem Geol, 1986, 56: 207－218[DOI]

21 Sun S, McDonough W. Chemical and isotopic systematics of oceanic basalts: for implications for mantle composition and processes. In: Saunders A, Norry M. eds. Magmatism in the Ocean Basin. Geol Soc Speci Publ, 1989, 42: 313－345

22 Sims K, DePolo D. Inferences about mantle magma sources from incompatible element concentration ratios in oceanic basalts. Geochim Cosmochim Acta, 1991, 61: 765－784[DOI]

23 Rehkamper M, Hofmann A W. Recycled ocean crust and sediment in Indian Ocean MORB. Earth Planet Sci Lett, 1997, 147: 93－106[DOI]

24 Hofmann A W. Mantle geochemistry: the message from oceanic volcanism. Nature, 1997, 385: 219－228[DOI]

25 Campbell I H, Implication of Nb/U, Th/U and Sm/Nd in plume magmas for the relationship between continental and oceanic crust formation and the development of the depleted mantle. Geochem Cosmochim Acta, 2002, 66: 1651－1661[DOI]

26 Hou G J, Zhu Y H, Zhang T P, et al. Geochemistry of basalts and analysis of tectonic setting in the Tuosuohu area, east Kunlun orogenic belt. Reg Geol Chin (in Chinese), 1998, Suppl.: 31－37

27 Kempton P D, Fitton J G, Saunders A D, et al. The Iceland plume in space and time: a Sr-Nd-Pb-Hf study of the North Atlantic Rifted margin. Earth Planet Sci Lett, 2000, 177: 255－271[DOI]

28 Wood A D, Joron J L, Treuil M, et al. Elemental and Sr isotope variations in basic lavas from Iceland and the surrounding ocean floor. Contri Mineral Petrol, 1979, 70: 319－339

29 Hofmann W A, White W M. Mantle plumes from ancient oceanic crust. Earth Plane Sci Lett, 1982, 57: 421－436[DOI]

30 Bijwaard H, Spakman W. Tomographic evidence for a narrow whole mantle plume below Iceland. Earth Planet Sci Lett, 1999, 166: 121－126[DOI]

31 Yale M M, Morgan J P. Asthenosphere flow model of hotspot-ridge interactions: a comparison of Iceland and Kerguelen. Earth Planet Sci Lett, 1998, 161: 45－56[DOI]

32 Weaver B L. The origin of oceanic basalt end-member compositions: trace element and isotopic constraints. Earth Planet Sci Lett, 1991, 104: 381－397[DOI]

33 Hofmann A W, Jochum K P, Seufert M. Nb and Pb in oceanic basalts: new constraints on mantle. Earth Planet Sci Lett, 1986, 79: 33－45[DOI]

34 Xu Z Q, Li H B, Yang J S, et al. A large transpression zone at the south margin of the east Kunlun Mountains and oblique subduction. Acta Geol Sin (in Chinese), 2001, 75: 156－164

35 Xia L Q, Xia Z C, Xu X Y. Middle-late Proterozoic volcanic rocks in the Southern Qinling Mountains and Precambrian continental rifting. Sci China Ser D-Earth Sci (in Chinese), 1996, 26: 237－243

36 Xia L Q, Xia Z C, Xu X Y. The confirmation of continental flood basalt of the Proterozoic Xixiang group in the south Qinling Mountains, and its geological implication. Geol Rev (in Chinese), 1996, 42: 513－522

37 Lai S C, Zhang G W, Pei X Z, et al. Geochemistry of the ophiolite and oceanic island basalt in the Kangxian-Pipasi- Nanping tectonic melange zone, south Qinling and their tectonic significance. Sci China Ser D-Earth Sci, 2004, 47(2): 128－137